



Bilateral Teleoperation with a Shared Design of Master and Slave Devices for Robotic Excavators in Agricultural Applications



Ilham Amani Rozaini, Nurul Emylia Natasya Ahmad Zakey, Mohd Hairi Mohd Zaman*, Mohd Faisal Ibrahim, Seri Mastura Mustaza and Asraf Mohamed Moubark

Department of Electrical, Electronic and Systems Engineering, Faculty of Engineering and Built Environment, Universiti Kebangsaan Malaysia, 43600 Bangi, Selangor, Malaysia

E-mail/Orcid Id:

IAR, ilhamamanir@gmail.com, <https://orcid.org/0009-0005-9202-6025>; NEAZ, natasyaemylia1@gmail.com, <https://orcid.org/0009-0007-7879-1964>; MHMZ, hairizaman@ukm.edu.my, <https://orcid.org/0000-0003-1678-4869>; MFI, faisal.ibrahim@ukm.edu.my, <https://orcid.org/0000-0002-5046-1206>; SMM, seri.mastura@ukm.edu.my, <https://orcid.org/0000-0002-7907-4197>; AMM, asrafmohamed@ukm.edu.my, <https://orcid.org/0000-0002-7596-5515>

Article History:

Received: 24th Sep., 2023
Accepted: 14th Nov., 2023
Published: 30th Nov., 2023

Keywords:

Kinematic, master-slave, robot arm, teleoperation

How to cite this Article:

Ilham Amani Rozaini, Nurul Emylia Natasya Ahmad Zakey, Mohd Hairi Mohd Zaman, Mohd Faisal Ibrahim, Seri Mastura Mustaza and Asraf Mohamed Moubark (2023). Bilateral Teleoperation with a Shared Design of Master and Slave Devices for Robotic Excavators in Agricultural Applications. *International Journal of Experimental Research and Review*, 35(Spl.), 119-127
DOI : <https://doi.org/10.52756/ijerr.2023.v35spl.011>

Abstract: The main objective of this study is to develop a shared design of master and slave devices for bilateral teleoperation mechanisms used for robotic excavators in agricultural applications. In robot teleoperation research, many potential applications within controlled and hazardous environments come to light. Robots, with their capacity for remote control by human operators through master devices, often employ the master-slave teleoperation approach. This strategy finds frequent use across manufacturing, construction, and agriculture industries. The master-slave system necessitates two interdependent components that collaboratively steer the robot in real time. However, challenges arise when manipulating the robot arm proves challenging due to structural differences between the master device (such as a joystick) and the slave device (the robot arm). A stable operational framework must be established for the robot to function optimally. This teleoperation system employs a master device to govern the actions of the slave device, a dynamic that heavily influences the operational complexity. Hence, the focal point of this study is to enhance the master-slave algorithm for teleoperation applications that rely on controlling robot arm movements. Despite the differing dimensions of the master and slave devices, they both share a common structure. The kinematic model bridging these components must be intelligible to ensure user-friendliness, facilitating effortless robot control. Calculating the robot arm's end effector movement and positioning involves employing the forward kinematics of the arm, determined through Denavit-Hartenberg parameters and transformation matrices. By mitigating communication delays between the master and slave devices using a technique centered around the robot arm's end effector position, the effectiveness of teleoperation can be significantly improved. Our designed robot arm attains 80% to 100% precision across joints. In summary, streamlining the robot arm's structure and minimizing delays offers a route to bolstering both stability and efficiency in robotic movement.

Introduction

Agricultural robots are designed to automate tasks on farms and plantations. This type of robot, known as a mobile manipulator, consists of three main components: a perception system with image processing, a planning and localization system for moving the mobile platform, and a control system for navigating the manipulator's end-effector (Mail et al., 2023). The increasing demand for

food worldwide and a shortage of human labor for traditional, labor-intensive farming have led to significant attention on these robots in recent years (Crowley, 2020).

Numerous efforts have been made to develop agricultural robots for various applications, including land preparation before planting, sowing and planting, plant treatment and protection, weeding and pest control, and harvesting and fruit picking. Substantial research on



harvesting and fruit-picking robots has focused on vegetables and small fruits (Kang et al., 2020; Wagner et al., 2021; You et al., 2020). These robots are generally designed for plants of lower height, as opposed to taller varieties like coconut and oil palm trees (Hudzari et al., 2020; Sowat et al., 2018).

Designing manipulators or robot arms for harvesting tall plants presents specific challenges due to height constraints (Chikelu, 2023; Firdaus et al., 2018; Hudzari et al., 2020; Khalid & Shuib, 2014). The manipulator's end-effector must be capable of reaching high positions, which can lead to instability if the mobile platform that supports the manipulator is not sufficiently heavy. On the other hand, if a heavy mobile platform is used to counteract instability, it raises concerns about the impact on the farmland. To address these requirements for both a high-end-effector position and overall stability, one approach is to retrofit a commercially available excavator, typically used for construction (Lee et al., 2019; Sun et al., 2020), with a custom manipulator, ultimately creating a robotic excavator for agricultural purposes.

Extensive research has been conducted on designing robotic excavators for various applications, including construction, mining, forestry, and others (Aguilar et al., 2020; Correa et al., 2022; Lee et al., 2019). The boom and arm of the excavator can be likened to a robot arm. Regarding control, robotic excavators operate in two modes: autonomous and teleoperated. With a master-slave configuration, teleoperation offers diverse capabilities for robot arms, enabling a range of operations (Rai et al., 2023). However, it's important to note that using a master-slave system for teleoperation does have certain limitations (Lampinen et al., 2021; Liu et al., 2019). In this framework, the master device directs the movement of processing devices, or slaves, in remote locations.

Master-slave teleoperation entails controlling a robot model through a remote control device or joystick. This method is frequently employed in high-stakes fields like aerospace (Liu et al., 2019), manufacturing (Lee et al., 2018; Zaman et al., 2020), oil and gas (Caiza et al., 2020), and beyond. Differences in the design of robot arm structures between master and slave devices can pose control challenges. For instance, in the industrial sector, the master robot arm is typically smaller than its slave counterpart (Huang et al., 2017). Conversely, the medical sector may have larger master devices than slave devices (Schäfer et al., 2019). This structural discrepancy complicates control for inexperienced operators, such as harvesting tasks in the agricultural sector, worsened by

asynchronous movement between master and slave devices (Pan et al., 2017).

For streamlined completion of tasks across distinct workspaces, employing a consistent design between slave and master devices within the master-slave system proves beneficial (Wang and Liu, 2022). Ensuring stability in robot movement entails precise and efficient control of position and orientation on large-size slave devices (Lawrence, 1993). Complex joint-flexible robot arms require composite adaptive control with teleoperation systems. Stability can be realized by adjusting the initial states of both master and slave devices. The compatibility of degrees of freedom between master and slave devices underpins two-way teleoperation stability (Tugal et al., 2017). Choosing an appropriate controller hinges on specific application demands, encompassing robot arm type, desired precision, accuracy levels and operating environment.

Differences in kinematic models between master and slave robot arms can impede operation and programming. Forward and inverse kinematic models are typically used, yet employing them across a master-slave teleoperation system with differing robot arms complicates the operational process. The robot kinematic model, which mathematically characterizes robot arm geometry and motion, can be described through the Denavit-Hartenberg (DH) convention and transformation matrix (Adzeman et al., 2020; Ting et al., 2021). DH convention models geometry and motion, while the transformation matrix is determined through DH parameters, describing relative orientation and position.

Real-time delays in the master and slave robot arm system impede operations. A significant delay mismatch between master and slave devices hampers processes. Delays can occur in various control system levels, including communication, algorithm processing, and physical movement of the slave device (Kebria et al., 2020; Yang et al., 2022). Reducing delay requires careful design and optimization of communication and control algorithms. A robust delay control technique based on position employs the robot arm's position information to balance delay and the control system. This method utilizes the robot arm's movement angle to determine end effector position.

Therefore, in this research, the master and slave devices share a design, degrees of freedom, and kinematic model, enhancing teleoperation for robot arms. Minimizing delays between master and slave devices remains crucial, ensuring optimal operation efficiency for the master-slave robot arm. The study aims to design a master-slave robot arm, develop its kinematic model, and

formulate a teleoperation algorithm with minimal delay to create a coherent teleoperation system.

Materials and Methods

This study encompasses a holistic approach to enhancing robot arm control through the master-slave algorithm for teleoperation applications. Figure 1 provides an overview of the research flow, including three sub-objectives for this study. The first sub-objective is to design a master device similar to the slave device, with different dimensions. Meanwhile, the second sub-objective is to derive the kinematic model for both the master and slave devices. Finally, a master-slave algorithm with minimal latency is developed.

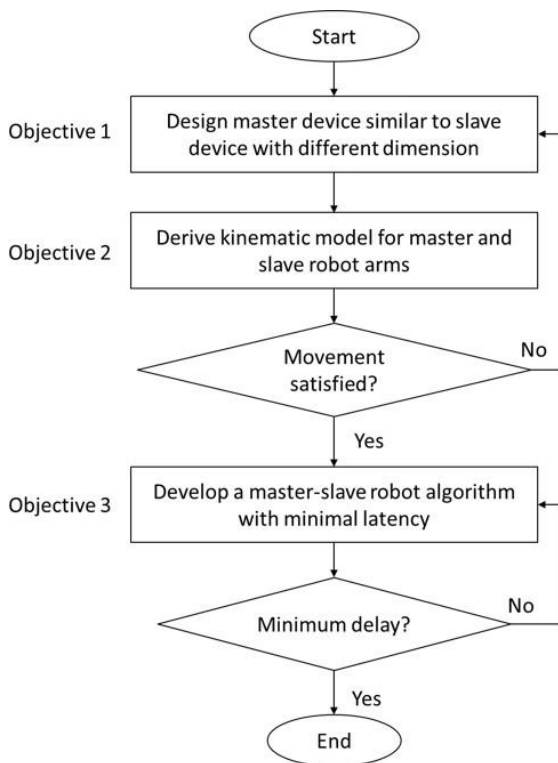


Figure 1. Research methodology

Robot Arm Design

The design of the robot arm is rooted in the OpenManipulator-X robot arm configuration, boasting four degrees of freedom (DOF), as depicted in Figure 2. The openManipulator-X robot arm was selected due to its open-source nature and suitability to represent an available excavator's boom and arm, as shown in Figure 3. The arm comprises joints 1, 2, 3, and 4, each rotating around the *x*, *y*, and *z* axes to emulate the excavator's movement depicted in Figure 3. Both master and slave devices share a design while differing in dimensions. The diagram illustrating this robot arm design, tailored for teleoperation applications, is presented in Figure 4. The master device is smaller and the slave device is larger, with dimensions outlined in Figure 2. Each joint of the

slave robot arm is connected to a corresponding potentiometer on the master device, totaling four sets of potentiometers due to the slave device's 4-DOF nature. Teleoperation is established to enable the master device to control the slave device using tools like a joystick.

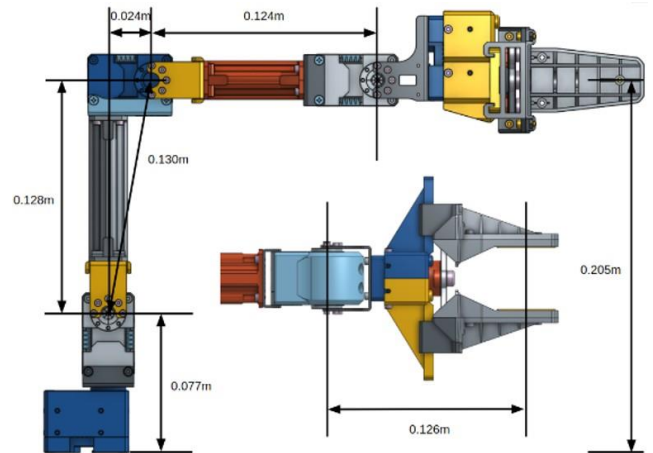


Figure 2. Dimensions of robot arm, model OpenManipulator-X, from Robotis company.



Figure 3. Available excavator with boom and arm mounted on a tractor (model B7001 from Kubota company)

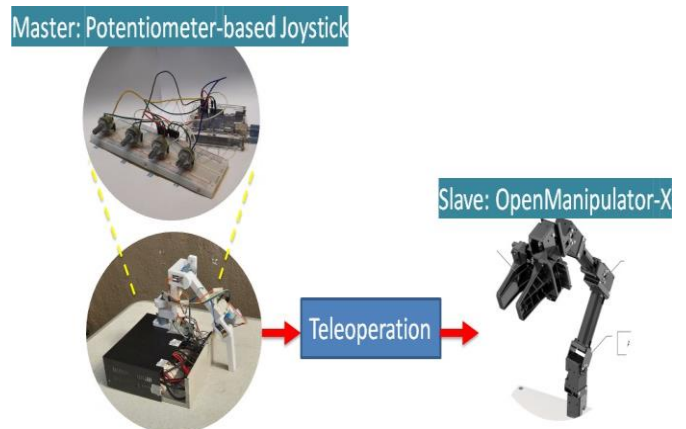


Figure 4. Shared design of master-slave teleoperation with the master device is a potentiometer-based joystick, while the slave device is OpenManipulator-X robot arm.

Forward kinematic model

The research employs the forward kinematic model using the Denavit-Hartenberg (DH) convention technique. The initial step involves determining system coordinates for each joint, followed by the derivation of the homogeneous transformation matrix for end-effector coordinates. A potentiometer on the master device gauges the movement angle of the OpenManipulator-X robot arm, thus determining forward kinematics. This movement is then applied to the slave device. The offset between joints L_2 and L_3 introduces an offset angle on the OpenManipulator-X robot arm, which is significant for DH parameter calculations. This involves trigonometric calculations, as depicted in Figure 5.

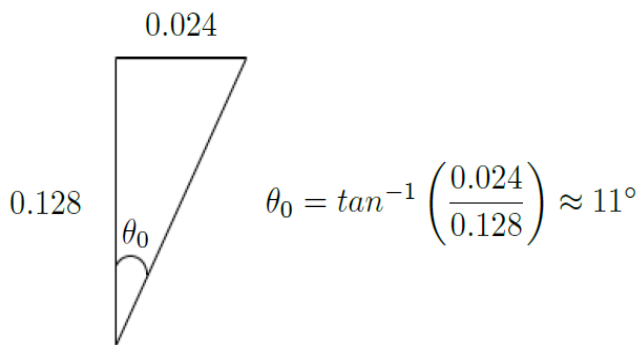


Figure 5. Joint L2 and L3 offset angle calculation

A comprehensive analysis of the robot arm's configuration leads to the development of a kinematic diagram illustrated in Figure 6. DH parameters (as detailed in Table 1) are then determined for the OpenManipulator-X robot arm.

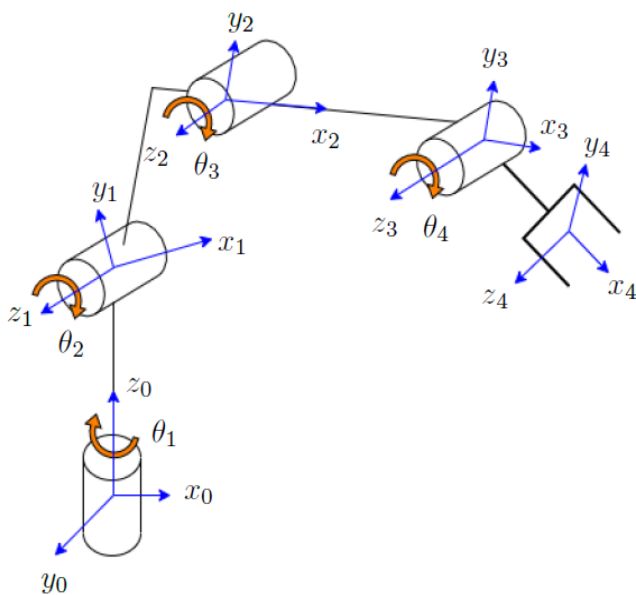


Figure 6. Kinematic diagram of OpenManipulator-X

Table 1. DH parameters of OpenManipulator-X

Joint	a_i (m)	α_i ($^\circ$)	d_i (m)	θ_i ($^\circ$)
1	0	90	0.077	θ_1
2	0.130	0	0	$\theta_2 - \theta_0 + 90^\circ$
3	0.124	0	0	$\theta_3 + \theta_0 - 90^\circ$
4	0.126	0	0	θ_4

Subsequently, the transformation matrix calculation is executed using the acquired DH parameters. Notably, the transformation matrix limit for the 4-DOF OpenManipulator-X robot arm is T^0 . Frame-specific matrix equations are written as follows,

$$T_i^{i-1} = \begin{bmatrix} \cos \theta_i & \sin \theta_i \cos \alpha_i & \sin \theta_i \sin \alpha_i & a_i \cos \alpha_i \\ \sin \theta_i & \cos \theta_i \cos \alpha_i & -\cos \theta_i \sin \alpha_i & a_i \sin \alpha_i \\ 0 & \sin \alpha_i & \cos \alpha_i & d_i \\ 0 & 0 & 0 & 1 \end{bmatrix} \dots \dots \dots (1)$$

$$T_1^0 = \begin{bmatrix} \cos \theta_1 & 0 & \sin \theta_1 & 0 \\ \sin \theta_1 & 0 & -\cos \theta_1 & 0 \\ 0 & 1 & 0 & d_1 \\ 0 & 0 & 0 & 1 \end{bmatrix} \dots \dots \dots (2)$$

$$T_2^1 = \begin{bmatrix} \cos \theta_2 & -\sin \theta_2 & 0 & a_2 \cos \theta_2 \\ \sin \theta_2 & \cos \theta_2 & 0 & a_2 \sin \theta_2 \\ 0 & 0 & 1 & 0 \\ 0 & 0 & 0 & 1 \end{bmatrix} \dots \dots \dots (3)$$

$$T_3^2 = \begin{bmatrix} \cos \theta_3 & -\sin \theta_3 & 0 & a_3 \cos \theta_3 \\ \sin \theta_3 & \cos \theta_3 & 0 & a_3 \sin \theta_3 \\ 0 & 0 & 1 & 0 \\ 0 & 0 & 0 & 1 \end{bmatrix} \dots \dots \dots (4)$$

$$T_4^3 = \begin{bmatrix} \cos \theta_4 & -\sin \theta_4 & 0 & a_4 \cos \theta_4 \\ \sin \theta_4 & \cos \theta_4 & 0 & a_4 \sin \theta_4 \\ 0 & 0 & 1 & 0 \\ 0 & 0 & 0 & 1 \end{bmatrix} \dots \dots \dots (5)$$

The end effector's position is derived by simplifying the transformation matrix equation, as expressed in the following equation.

$$T_4^0 = T_1^0 \cdot T_2^1 \cdot T_3^2 \cdot T_4^3 = \begin{bmatrix} n_x & o_x & a_x & p_x \\ n_y & o_y & a_y & p_y \\ n_z & o_z & a_z & p_z \\ 0 & 0 & 0 & 1 \end{bmatrix} \dots (6)$$

The resultant position vector (p_x, p_y, p_z) , encompasses end effector coordinates (x, y, z) . The master device's potentiometer and the slave device (the OpenManipulator-X robot arm) facilitate teleoperation within the same workspace due to a shared degree of freedom design.

Position-Based Delay Control

Position-based delay control is elucidated in Figure 7. Calculating delay time entails issuing a command from

the master device and then calculating the slave device's time to complete the command. Compensation position is subsequently determined based on the delay, predicting future arm position by accounting for current velocity. The calculated compensation position augments the command position, forming the new one. This guides the slave device's execution of the command with real-time monitoring and lag compensation updates. Movement accuracy, precision of final angles, and time delay are calculated as follows:

$$Accuracy = \left[1 - \frac{(y_m - x_m) - (y_s - x_s)}{(y_m - x_m)} \right] \times 100\% \dots\dots\dots(7)$$

with $x_m, x_s, y_m,$ and y_s representing the initial and final positions of the master and slave robots, respectively.

$$Precision = \left[1 - \frac{\theta_{ref} - \theta_f}{\theta_{ref}} \right] \times 100\% \dots\dots\dots(8)$$

with θ_{ref} signifies the reference angle, while θ_f denotes the final angle.

$$Delay = (t_{fm} - t_{im}) - (t_{fs} - t_{is}) \dots\dots\dots(9)$$

with $t_{im}, t_{is}, t_{fm},$ and t_{fs} corresponding to the initial and final times taken by the master and slave robots.

Result and Discussion

This section presents the outcomes of our investigation into robot arm control via the master-slave algorithm for teleoperation. We delve into the design of a master-slave system, employing forward kinematic modeling for the OpenManipulator-X robot arm and minimizing delays.

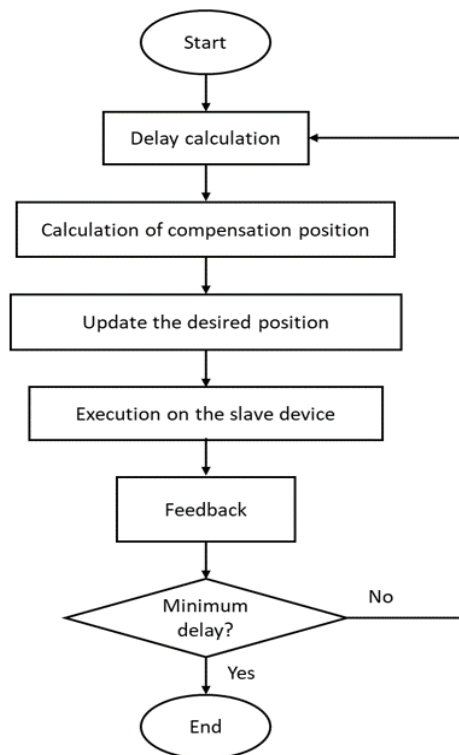


Figure 7. Delay measurement flowchart

Master-Slave Shared Design

To emulate the OpenManipulator-X robot arm, we have integrated its specifications into MATLAB for simulation. Utilizing potentiometers, we transform voltage readings into robot joint angles, steering the arm's movement. The simulation revolves around a master-slave system, where the master device (potentiometer) dictates the slave device (robot arm) motion. Designing for consistency, we employ four potentiometers corresponding to the 4-DOF nature of OpenManipulator-X. This uniform structure is visualized in Figure 4.

The potentiometer data is transmitted through Arduino and processed in MATLAB Simulink to ensure conformity within OpenManipulator-X's joint angle range. Subsequently, this processed data drives the MATLAB-designed robot, characterized by OpenManipulator-X's specifications, as depicted in Figure 8. Besides, Figure 9 shows the corresponding Simulink Multibody program.

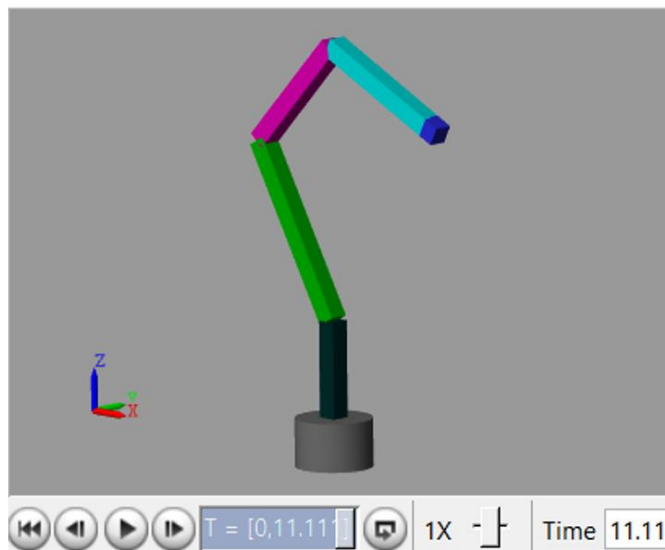


Figure 8. OpenManipulator-X design in MATLAB

Forward Kinematic Model

MATLAB is harnessed to develop the forward kinematic model for our master-slave robot arm. We analytically calculate DH parameters and the transformation matrix through MATLAB programming, simplifying end effector coordinate determination. We apply similar inputs directly to the potentiometer for robot arm implementation in MATLAB experiments. The initial OpenManipulator-X kinematic model is outlined in Table 2.

Table 2. Initial OpenManipulator-X end effector coordinate

Axis Position	Coordinate
x-axis	0.2748
y-axis	0
z-axis	0.2046

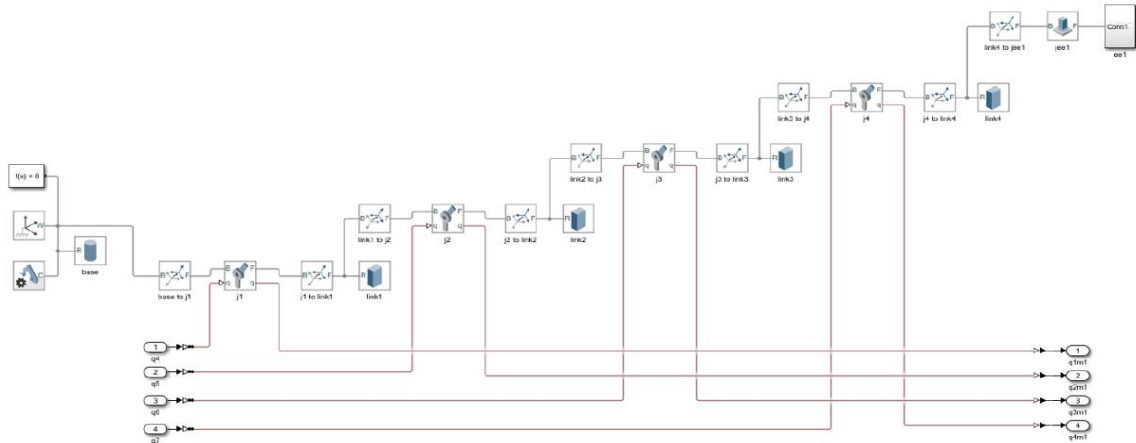


Figure 9. MATLAB Simulink program to control OpenManipulator-X

We validate our model by comparing analytical calculations with MATLAB simulations. Ten randomly chosen input angles yield corresponding end effector coordinates, visualized in Figure 10 for the *x*-axis, Figure 11 for the *y*-axis, and Figure 12 for the *z*-axis. These end effector coordinates mimic the harvesting tasks in agricultural applications.

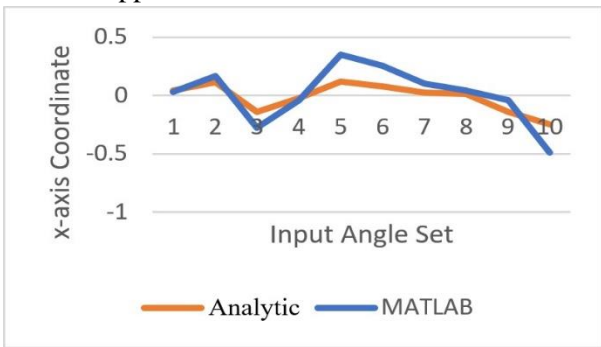


Figure 10. x-axis end effector coordinate

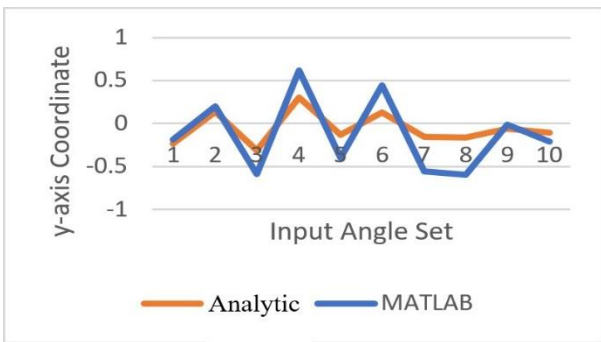


Figure 11. y-axis end effector coordinate

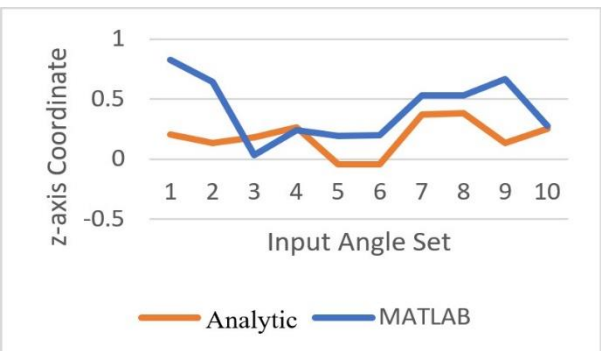


Figure 12. z-axis end effector coordinate

Though exhibiting significant magnitude differences, the analytical and MATLAB end effector positions reside within the same workspace. However, discrepancies stem from factors like instrumentation error due to varying electronic component limits among potentiometer types. Calibration is paramount for accuracy, considering the potentiometer's sensitivity to even minor resistance changes. The findings can be utilized when retrofitting a commercially available excavator (as the slave device), typically used for construction, with a custom manipulator (as the master device), ultimately creating a safe robotic excavator for agricultural purposes. Besides, since this work is limited to the 4-DOF robot arm, further research with higher DOF needs to be studied in the future.

Optimum Teleoperation Delay

Precision, accuracy, and time delay are pivotal in teleoperation calculations. Both master and slave devices contribute to this study, interacting for motion synchronization. Accuracy, represented in Figure 13, gauges parallelism between master and slave robot arm movements, achieving 80% to 100% alignment. Simulation complexities necessitate a minute time step for heightened accuracy, even though this increases simulation intricacy.

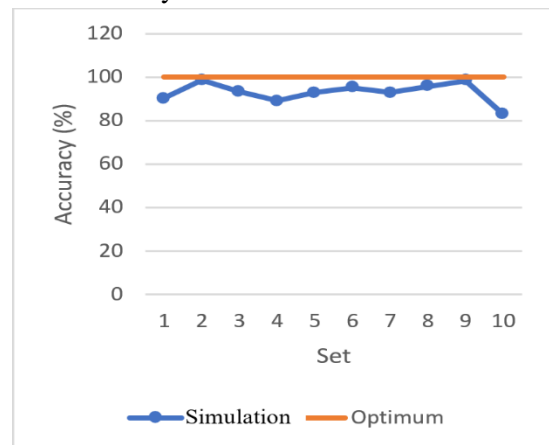


Figure 13. Accuracy of master-slave robot arm movements

Precision, imperative for precise robot arm control, ensures accurate end effector positioning and trajectory tracking, as depicted in Figure 14. Our designed robot arm attains 80% to 100% precision across joints, underscoring its capability to accomplish tasks and attain specific positions. Time delays, inherent in master-slave teleoperation, stem from data connectivity. Calculations that emphasize accuracy, precision, and time delay, which involve master and slave devices, ensuring harmonious motion. Teleoperation accuracy and precision reside between 80% and 100%, influenced by real-time data acquisition, hardware limitations, and simulation intricacies. Figure 15 visualizes the time delay, ranging from -0.03s to 0.05s, impacting the efficiency of robot movement.

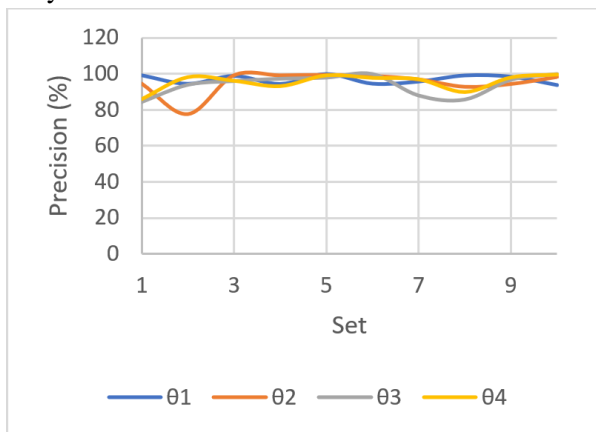


Figure 14. Precision of final angle to reference angle for each joint

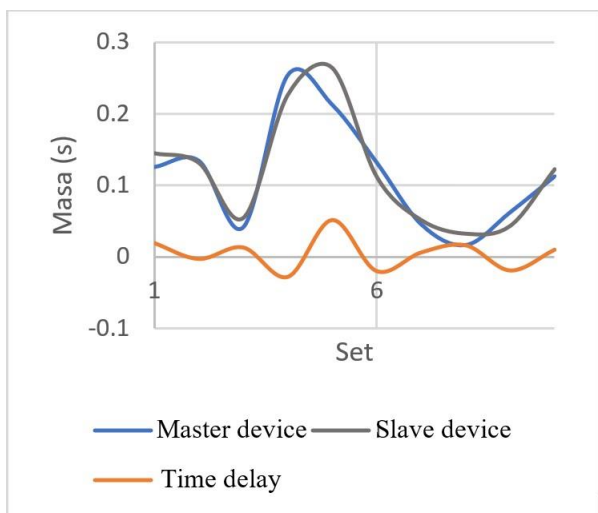


Figure 15. Time delay in master-slave robot arm movements

Conclusion

This research introduces an effective master-slave teleoperation algorithm for robot arms. We enhance operational efficiency by adopting uniform design principles, implementing forward kinematic modeling, and minimizing delays. The potential for real-time data transmission via the Internet of Things (IoT) could

revolutionize teleoperation, particularly in dynamic fields like agriculture, mitigating labor challenges.

Acknowledgement

This work was financially supported by Universiti Kebangsaan Malaysia (grant no. GUP-2021-024).

Conflict of Interest

The authors declare no conflict of interest.

References

- Adzeman, M. A. M., Zaman, M. H. M., Nasir, M. F., Ibrahim, M. F., & Mustaza, S. M. (2020). Kinematic modeling of a low cost 4 DOF robot arm system. *International Journal of Emerging Trends in Engineering Research*, 8(10), 6828–6834. <https://doi.org/10.30534/ijeter/2020/328102020>
- Aguiar, A. S., Santos, F. N. Dos, Cunha, J. B., Sobreira, H., & Sousa, A. J. (2020). Localization and mapping for robots in agriculture and forestry: A survey. *Robotics*, 9(4), 97. <https://doi.org/10.3390/robotics9040097>
- Caiza, G., Garcia, C. A., Naranjo, J. E., & Garcia, M. V. (2020). Flexible robotic teleoperation architecture for intelligent oil fields. *Heliyon*, 6(2020), e03833. <https://doi.org/10.1016/j.heliyon.2020.e03833>
- Chikelu, P. O. (2023). Model design and development of a telescopic palm fruit harvester. *Modern Mechanical Engineering*, 13(01), 1–20. <https://doi.org/10.4236/mme.2023.131001>
- Correa, M., Cárdenas, D., Carvajal, D., & Ruiz-del-Solar, J. (2022). Haptic teleoperation of impact hammers in underground mining. *Applied Sciences*, 12(3), 1428. <https://doi.org/10.3390/app12031428>
- Crowley, M. (2020). Foreign labor shortages in the Malaysian palm oil industry: Impacts and recommendations. *Asian Journal of Agriculture and Development*, 17(2), 1–18. <https://doi.org/10.37801/ajad2020.17.2.1>
- Firdaus, M., Aziz, A., Firdaus, M., & Aziz, A. (2018). Mechanization in oil palm harvesting. *International Journal of Academic Research in Business & Social Sciences*, 8(5), 247–256. <https://doi.org/10.6007/IJARBS/v8-i5/4098>
- Huang, L., Yamada, H., Ni, T., & Li, Y. (2017). A master-slave control method with gravity compensation for a hydraulic teleoperation construction robot. *Advances in Mechanical Engineering*, 9(7). <https://doi.org/10.1177/1687814017709701>

- Hudzari, M., Bakar, M. A., & Mohd Sabir, M. S. (2020). Conceptual development of automated harvester for tall oil palm tree. *Advances in Agricultural and Food Research Journal*, 1(2), a0000151. <https://doi.org/10.36877/aafrj.a0000151>
- Kang, H., Zhou, H., Wang, X., & Chen, C. (2020). Real-time fruit recognition and grasping estimation for robotic apple harvesting. *Sensors*, 20(19), 1–15. <https://doi.org/10.3390/s20195670>
- Kebria, P. M., Khosravi, A., Nahavandi, S., Shi, P., & Alizadehsani, R. (2020). Robust adaptive control scheme for teleoperation systems with delay and uncertainties. *IEEE Transactions on Cybernetics*, 50(7), 3243–3253. <https://doi.org/10.1109/TCYB.2019.2891656>
- Khalid, M. R., & Shuib, A. R. (2014). Field evaluation of harvesting machines for tall oil palms. *Journal of Oil Palm Research*, 26(2), 125–132. [zer](https://doi.org/10.1109/TCST.2021.3091314)
- Lampinen, S., Koivumaki, J., Zhu, W. H., & Mattila, J. (2021). Force-sensor-less bilateral teleoperation control of dissimilar master-slave system with arbitrary scaling. *IEEE Transactions on Control Systems Technology*, 30(3), 1037–1051. <https://doi.org/10.1109/TCST.2021.3091314>
- Lawrence, D. A. (1993). Stability and transparency in bilateral teleoperation. *IEEE Transactions on Robotics and Automation*, 9(5), 624–637. <https://doi.org/10.1109/70.258054>
- Lee, J., Kim, B., Sun, D., Han, C., & Ahn, Y. (2019). Development of unmanned excavator vehicle system for performing dangerous construction work. *Sensors*, 19(22), 4853. <https://doi.org/10.3390/s19224853>
- Lee, J.-D., Li, W.-C., Shen, J.-H., & Chuang, C.-W. (2018). Multi-robotic arms automated production line. *2018 4th International Conference on Control, Automation and Robotics (ICCAR)*, 26–30. <https://doi.org/10.1109/ICCAR.2018.8384639>
- Liu, G., Geng, X., Liu, L., & Wang, Y. (2019). Haptic based teleoperation with master-slave motion mapping and haptic rendering for space exploration. *Chinese Journal of Aeronautics*, 32(3), 723–736. <https://doi.org/10.1016/j.cja.2018.07.009>
- Mail, M. F., Maja, J. M., Marshall, M., Cutulle, M., Miller, G., & Barnes, E. (2023). Agricultural harvesting robot concept design and system components: A review. *AgriEngineering*, 5(2), 777–800. <https://doi.org/10.3390/agriengineering5020048>
- Pan, C., Liu, X., & Jiang, W. (2017). Design and synchronization control of heterogeneous robotic teleoperation system. *2017 Chinese Automation Congress (CAC)*, pp. 406–410. <https://doi.org/10.1109/CAC.2017.8242801>
- Rai, A., Kundu, K., Dev, R., Keshari, J. P., & Gupta, D. (2023). Design and development Virtual Doctor Robot for contactless monitoring of patients during COVID-19. *International Journal of Experimental Research and Review*, 31, 42–50. <https://doi.org/10.52756/10.52756/ijerr.2023.v31sp1.005>
- Schäfer, M. B., Stewart, K. W., & Pott, P. P. (2019). Industrial robots for teleoperated surgery - A systematic review of existing approaches. *Current Directions in Biomedical Engineering*, 5(1), 153–156. <https://doi.org/10.1515/cdbme-2019-0039>
- Sowat, S. N., Ishak, W., Ismail, W., Mahadi, M. R., Bejo, S. K., Saufi, M., & Kassim, M. (2018). Trend in the development of oil palm fruit harvesting technologies in Malaysia. *Jurnal Teknologi*, 80(2), 83–91. <https://doi.org/10.11113/jt.v80.11298>
- Sun, D., Baek, I., Hwang, S., Lee, S., Lee, S. K., Jang, S., Ji, C., Han, J., & Han, C. (2020). Sensor-based straight-line control of the end-point of a typical retrofitted hydraulic excavator. *Automation in Construction*, 120, 103385. <https://doi.org/10.1016/j.autcon.2020.103385>
- Ting, H. Z., Zaman, M. H. M., Ibrahim, M. F., & Moubark, A. M. (2021). Kinematic analysis for trajectory planning of open-source 4-DoF robot arm. *International Journal of Advanced Computer Science and Applications*, 12(6), 769–777. <http://dx.doi.org/10.14569/IJACSA.2021.0120690>
- Tugal, H., Carrasco, J., Falcon, P., & Barreiro, A. (2017). Stability analysis of bilateral teleoperation with bounded and monotone environments via Zames–Falb multipliers. *IEEE Transactions on Control Systems Technology*, 25(4), 1331–1344. <https://doi.org/10.1109/TCST.2016.2601289>
- Wagner, N., Kirk, R., Hanheide, M., & Cielniak, G. (2021). Efficient and robust orientation estimation of strawberries for fruit picking applications. *2021 IEEE International Conference on Robotics and Automation (ICRA)*, 13857–13863. <https://doi.org/10.1109/ICRA48506.2021.9561848>
- Wang, J., & Liu, J. (2022). Bilateral coordination quantisation control for master-slave flexible manipulators based on PDE dynamic model. *International Journal of Control*, 95(8), 2279–

2292.

<https://doi.org/10.1080/00207179.2021.1906448>

Yang, X., Yan, J., Hua, C., & Guan, X. (2022). Position measurement based slave torque feedback control for teleoperation systems with time-varying communication delays. *IEEE/CAA Journal of Automatica Sinica*, 10(2), 388-402. <https://doi.org/10.1109/JAS.2022.106076>

You, A., Sukkar, F., Fitch, R., Karkee, M., & Davidson, J. R. (2020). An efficient planning and control framework for pruning fruit trees. *2020 IEEE*

International Conference on Robotics and Automation (ICRA), 3930–3936.

<https://doi.org/10.1109/ICRA40945.2020.9197551>

Zaman, M. H. M., Ibrahim, M. F., Zainal, N., & Nasir, M. F. (2020). Dual-arm robot with mobile robot platform with master-slave configuration for teleoperation application. *International Journal of Advanced Trends in Computer Science and Engineering*, 9(1.4), 685–688.

<https://doi.org/10.30534/ijatcse/2020/9691.42020>

How to cite this Article:

Ilham Amani Rozaini, Nurul Emylia Natasya Ahmad Zakey, Mohd Hairi Mohd Zaman, Mohd Faisal Ibrahim, Seri Mastura Mustaza and Asraf Mohamed Moubark (2023) Bilateral Teleoperation with a Shared Design of Master and Slave Devices for Robotic Excavators in Agricultural Applications. *International Journal of Experimental Research and Review*, 35(Spl.),119-127.

DOI : <https://doi.org/10.52756/ijerr.2023.v35spl.011>



This work is licensed under a Creative Commons Attribution-NonCommercial-NoDerivatives 4.0 International License.